Developments of high rate dissolved air flotation for drinking water treatment

James K. Edzwald

ABSTRACT

Since the mid 1990s there has been a large increase in the hydraulic loading rates used to design dissolved air flotation (DAF) facilities for drinking water applications. High rate DAF processes are now available at loading rates of 20 to 40 m h^{-1}. These high rate systems have a smaller plant footprint compared to conventional systems. The paper examines bubble and floc-bubble rise rates, and how the simple theory relating these rise rates to the hydraulic loading of the DAF separation zone is inadequate. It is shown for high rate systems that the flow through the separation zone is stratified and must be accounted for in relating separation zone efficiency to the hydraulic loading and bubble or floc-bubble rise rates. A conceptualized stratified flow model is used to explain why DAF tanks can be designed with hydraulic loadings >20 m h^{-1}.

Key words | bubble rise rates, dissolved air flotation, drinking water, floc-bubble rise rates, high rate flotation, separation zone

James K. Edzwald (corresponding author)
Department of Civil and Environmental Engineering,
Clarkson University,
Potsdam,
NY 13699-5710,
USA
E-mail: *jedzwald@clarkson.edu*

NOMENCLATURE

A	gross tank area
A_{sz}	separation zone surface area
d_b	bubble diameter
d_f	floc diameter
d_{raw}	raw water particle diameter
d_{fb}	diameter of the floc-bubble aggregate
C_b	air or bubble mass concentration in contact zone
C_r	air mass concentration in recycle flow in equilibrium with saturator air at saturator pressure
$C_{s,air}$	air mass concentration at saturation in water for atmospheric pressure
e	saturator efficiency
g	gravitational constant (9.806 m/sec^2)
k	air deficit concentration
K	factor to account for shape effects on drag
n_b	bubble number concentration
n_{raw}	raw water particle number concentration
N	number of bubbles attached to a floc
Q	through rate flow rate
Q_r	recycle flow rate
R	recycle rate or ratio
v_b	the bubble rise velocity
$v_{clar\text{-}hl}$	clarification area hydraulic loading
v_{fb}	the floc-bubble rise velocity
$v_{sz\text{-}hl}$	separation zone hydraulic loading
$v_{nom\text{-}hl}$	nominal tank hydraulic loading
t_{cz}	contact zone hydraulic detention time
α_{pb}	particle-bubble attachment efficiency
ρ_b	air bubble density
ρ_f	floc density
ρ_{fb}	floc-bubble density
ρ_w	water density
μ_w	water dynamic viscosity
Φ_b	air or bubble volume concentration
Φ_{raw}	raw water particle volume concentration
π	mathematical constant (3.14)

doi: 10.2166/aqua.2007.013

INTRODUCTION

Dissolved air flotation (DAF) has been used to treat drinking water supplies for over 45 years. The process was first used in Scandinavia and South Africa, and over the last 25 years has

Downloaded from https://iwaponline.com/aqua/article-pdf/56/6-7/399/401152/399.pdf
by guest

seen increasing and widespread use around the world. It is a better clarification process than sedimentation for treating reservoir supplies and supplies containing natural color. In short, it is more efficient than settling for removing low density particles either initially in the raw water or produced through precipitation from metal coagulants.

In the early years, the design and operation of DAF plants were based largely on experience and pilot plant data. Our understanding of DAF has been greatly improved through the development of fundamental principles and models. Some selected contributions are those of Edzwald (Edzwald *et al.* 1990a, 1995), Tambo (Tambo *et al.* 1986; Fukushi *et al.* 1995, 1998; Matsui *et al.* 1998), and Han (2002). Haarhoff & Edzwald (2004) summarized the state of knowledge regarding modelling the contact and separation zones of the DAF process, and they identified subjects that need additional research. The fundamental research conducted over the last 25 years serves as a foundation for technological developments in DAF. DAF plants until about 1990 were designed with long pretreatment flocculation times and the DAF tank was sized with low hydraulic loading rates of about 5 to 10 $m\,h^{-1}$. In the last 15 years, there has been a trend of reducing the flocculation detention time and increasing the hydraulic loading rate.

The purpose of this paper is to describe the developments of high rate DAF processes. The scope of the paper follows: firstly, a brief description of a DAF water plant is presented; secondly, the properties and concentrations of particles, floc particles or simply "flocs", and bubbles are summarized; thirdly, the theoretical rise velocities of bubbles and floc-bubble aggregates are presented; fourthly, some pilot data are summarized showing that DAF processes are feasible with hydraulic loadings greater than the theoretical rise velocities, and some high rate DAF processes now available are briefly described; fifthly, a modification of the theory is made that relates rise velocities to the DAF tank hydraulic loading for the removal of bubbles and aggregates.

DESCRIPTION OF DISSOLVED AIR FLOTATION

Figure 1 is a process schematic diagram for a DAF drinking water plant. Coagulation and flocculation are required pretreatment processes. Coagulation is a chemical addition step. The coagulants used most often in water treatment are aluminum and ferric salts. Coagulation has two purposes: to destabilize particles present in the raw water and to convert

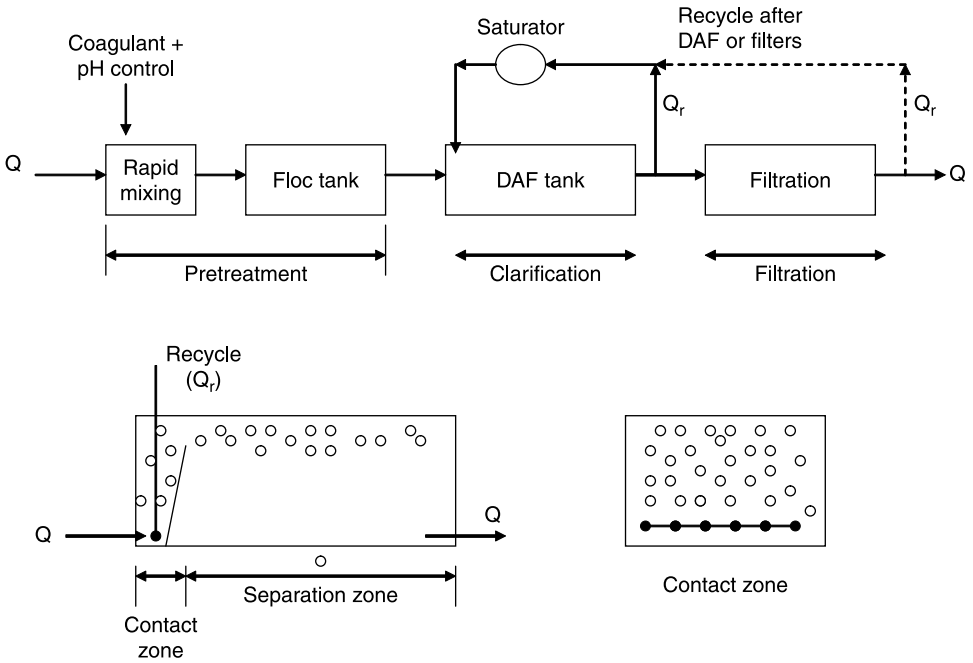

Figure 1 | Process schematic of a DAF water plant.

Downloaded from https://iwaponline.com/aqua/article-pdf/56/6-7/399/401152/399.pdf
by guest

dissolved natural organic matter into particles. The latter purpose, over the last 25 years, has become an essential part of water treatment used to remove as much dissolved organic carbon as feasible through coagulation. The chemistry of coagulation involves selecting proper dosing and pH conditions to produce particles – originally in the raw water and new particles produced through metal coagulant precipitation – that can forms flocs in the flocculation tank, and ultimately to attach bubbles to flocs in the DAF tank. The goal of coagulation chemistry then, is to produce particles with little or no net electrical surface charge and with a relatively hydrophobic character. The chemistry of coagulation for sedimentation and DAF plants is similar, so that coagulant dosages and pH conditions are identical for forming flocs. An exception is that for some water types, especially those of low to moderate turbidities, sedimentation plants may require higher coagulant dosages so as to increase flocculation kinetics and produce flocs large enough to settle rapidly.

The flocculation step involves mixing the water to induce collisions among particles and precipitated particles from metal coagulants yielding flocs. The sizes of flocs in the influent to the DAF tank affects greatly the collisions among flocs and bubbles in the DAF tank contact zone and subsequently, the rise velocities of flocs with attached bubbles in the DAF tank separation zone. The flocs with attached bubbles are called floc-bubble aggregates. Flocculation is used in both sedimentation and DAF plants, but their objectives differ. When settling follows flocculation, the goal is to produce large flocs capable of settling at a fairly rapid rate. Flocs with sizes of 100 μm and greater are required to produce reasonable settling rates. Proper floc sizes for DAF differs, especially in treating reservoir supplies with low density particles and little mineral turbidity. For treating these type supplies, the optimum floc size for the DAF contact zone is 10 s of microns determined from modelling, laboratory, and pilot plant data (Edzwald *et al.* 1990a; Edzwald & Wingler 1990b; Edzwald *et al.* 1992; Edzwald 1995). It has been demonstrated through extensive pilot plant data that flocculation times of 5–10 min are adequate (Valade *et al.* 1996; Edzwald *et al.* 1999). Over the last 10 to 15 years, many full-scale plants around the world have been placed into operation with short flocculation times; for example, Crossley & Valade (2006) reported that a new plant for New York City (design flow of $1.1 \times 10^6\ m^3\ d^{-1}$) will have a flocculation time of only 5 min.

The DAF tank is divided into two sections with different functions as illustrated at the bottom of Figure 1. There is a section at the front end that is baffled, called the contact zone, where floc particles are introduced and contacted with air bubbles. Here, collisions occur among bubbles and floc particles. If the floc particles are prepared properly via coagulation with respect to their surface chemistry, then bubbles colliding with the flocs may attach yielding floc-bubble-aggregates. The water carrying the suspension of bubbles, flocs, and aggregates flows to the second section of the tank, called the separation zone. Here, bubbles not attached to flocs and floc-bubble-aggregates may rise to the surface of the tank. The float layer at the surface of the tank consists of a mixture of bubbles and floc particles attached to bubbles. In drinking water applications, this froth is called the float. Over time, this float layer is concentrated producing a sludge that is collected and removed from the tank. Clarified water, often referred to as the subnatant, is withdrawn from the bottom of the tank. In a standard plant, DAF and granular media filtration are separated horizontally. In some DAF plant applications, DAF is placed vertically above the filters.

Air is dissolved in a recycle flow by adding air under pressure in a saturator. The recycle rate (R) is defined by Equation (1), where Q is the plant through-put flow and Q_r is the recycle flow. Typical recycle rates are 8 to 12%. Saturator pressures are typically between 400 and 600 kPa. The recycle flow is injected through nozzles or special valves at the bottom entrance of the contact zone. Microbubbles of 10 to 100 μm are produced, and give a milky appearance to the water; hence the name *white water*.

$$R = \frac{Q_r}{Q} \tag{1}$$

Some introductory comments are made here about the hydraulic loading of DAF tanks. Most often, the nominal hydraulic loading (v_{nom-hl}) is used to describe DAF loading rate. It is defined by Equation (2). Note that this definition ignores the recycle flow and uses the gross plan tank area (A) of the contact and separation zones.

$$v_{nom-hl} = \frac{Q}{A} \tag{2}$$

The removal of bubbles and floc-bubble aggregates occurs in the separation zone. The separation of bubbles

Downloaded from https://iwaponline.com/aqua/article-pdf/56/6-7/399/401152/399.pdf
by guest

and aggregates depends on their rise velocities relative to the hydraulic loading for the separation zone; they must be greater. Therefore, the separation zone performance should be described in terms of the separation zone hydraulic loading (v_{sz-hl}) using the sum of the plant throughput flow and the recycle flow divided by the separation zone plan area (A_{sz}) as presented by Equation (3).

$$v_{sz-hl} = \frac{Q + Q_r}{A_{sz}} \tag{3}$$

A major part of this paper addresses later the fundamentals of rise velocities, and modification of the traditional Hazen theory approach relating hydraulic loadings to rise velocities to explain developments of high rate DAF processes.

PARTICLE AND BUBBLE SUSPENSIONS

Some comparisons are made in this section among the concentrations of raw water particles, flocs in the DAF tank influent, and bubble concentrations in the DAF tank contact zone. The concentrations are presented on both a number and volume basis. The applications considered are in treating reservoir type water supplies. This means that the raw water mineral turbidity is low and not important compared to low density particles present in the reservoir. These particles are mostly organic in nature and are attributed to algae, bacteria, protozoa and the like.

The suspended solids concentration on a mass basis is also considered low, which is true for most reservoir supplies. Expressed on a volume basis (Φ_{raw}), two cases are considered of 1 and 10 ppm. The raw water particle concentrations (n_{raw}) are calculated from Equation (4) for two particle size cases of 1 and 10 μm. The results are summarized in Table 1. These calculations show that particle number concentrations can vary over a wide range, and depend significantly on the raw water particle size. Actual measurements using electronic particle counters are limited usually to sizes greater than 2 μm. Some particle counters can detect sizes of 1 μm, and show a large number of particles at this size. In short, n_{raw} of at least 10^6 and often exceeding 10^7 particles per L are reasonable values. The number concentration changes with coagulation and flocculation, and is of interest with respect to DAF.

$$n_{raw} = \frac{\Phi_{raw}}{\pi (d_{raw})^3/6} \tag{4}$$

Alum coagulation is usually practiced at dosing and pH conditions called sweep floc meaning that the dissolved aluminum added exceeds the solubility of $Al(OH)_3(s)$. Precipitation occurs producing additional solids. For alum dosing (as Al) of 2.5 to 5 mg L^{-1}, the solids added on a volume basis are in the range of 6.5 to 13 ppm. A value of 10 ppm is used for illustrative purposes. Adding the precipitated solids from the coagulant to the raw water solids, the floc volume

Table 1 | Raw water before alum addition and floc particle concentrations after alum addition (assumed alum adds 10 ppm of particles)

	Raw Water					
	Φ_{raw} of 1 ppm			**Φ_{raw} of 10 ppm**		
Particle diameter (μm)	1	10		1	10	
n_{raw} (# L^{-1})	1.9×10^9	1.9×10^6		1.9×10^{10}	1.9×10^7	
	Flocs					
	Φ_{floc} of 11 ppm			**Φ_{floc} of 21 ppm**		
Floc diameter (μm)	5	10	50	5	10	50
n_{floc} (# L^{-1})	1.7×10^8	2.1×10^7	1.7×10^5	3.2×10^8	4.0×10^7	3.2×10^5

Downloaded from https://iwaponline.com/aqua/article-pdf/56/6-7/399/401152/399.pdf
by guest

concentrations are now 11 and 21 ppm as indicated in Table 1. Flocculation increases the particle size, so after flocculation we consider floc sizes of 5, 10, and 50 μm. The calculations for floc number concentrations (n_{floc}) are summarized at the bottom of Table 1. If the particles are dominated with small flocs of say 5 μm, then the floc particle concentrations are high exceeding 10^8 flocs per L. If the flocculation process grows flocs into mean sizes exceeding 10 s of μm, then the floc concentrations decrease to say 10^6 flocs per L. Of course, particles do not flocculate into perfect spheres, which are assumed in the simple calculations here. They form different shapes and have an internal porous structure, or fractal geometry. Haarhoff & Edzwald (2001, 2004) have examined in detail the effects of flocculation on floc density and floc number concentration for a range of fractal dimensions. While floc density is highly dependent on the extent of flocculation (floc size compared to primary particle size) and the fractal dimension, the number concentration is not affected much so that the simple calculations presented in Table 1 suffice.

The mass concentration of air released in the contact zone (C_b) is calculated from Equation (5), which is obtained from a mass balance accounting for the saturator efficiency (e), the air in the recycle flow in equilibrium with saturator air (C_r), the saturation concentration of air ($C_{s,air}$) in water at 101.3 kPa, the recycle rate (R), and k which accounts for any air deficit concentration in the influent flocculated water to the DAF tank. The two main variables for controlling C_b are the saturator pressure, which affects C_r, and the recycle rate (R). C_b is controlled primarily in practice through R, since for a particular plant the saturator pressure is not changed very much. The bubble volume (Φ_b) and number (n_b) concentrations are calculated from Equations (6) and (7).

$$C_b = \frac{|e(C_r - C_{s,air})R - k|}{1 + R} \tag{5}$$

$$\Phi_b = \frac{C_b}{\rho_b} \tag{6}$$

$$n_b = \frac{\Phi_b}{\pi (d_b)^3/6} \tag{7}$$

Bubble suspension concentrations are summarized in Table 2 for a common range of recycle rates and typical saturator design conditions. A mean bubble size of 60 μm is assumed for the contact zone (Haarhoff & Edzwald 2004). It is instructive to compare the bubble volume and number concentrations to the floc volume and number concentrations entering DAF (latter values from Table 1). A comparison is made for a recycle ratio of 10%. The results are presented in Table 3 for three mean floc sizes. The results show that bubble volumes are much greater than floc volumes. This provides for the potential reduction in the density of floc-bubble aggregates assuming sufficient bubble attachment to flocs occurs. For flotation to occur, the bubble numbers must exceed the floc concentrations – i.e., there has to be at least one bubble attached to every floc. The results in Table 3 show that if all flocs are small (5 μm and less), then there may be an insufficient number of bubbles. Increasing flocs to sizes greater than 10 μm insures bubbles exceed floc particles. Haarhoff & Edzwald (2004) examined this problem in greater detail accounting for fractal floc geometry, and also concluded that to have an excess of air bubbles, particles should grow in flocculation to average floc sizes of at least 10 μm.

Table 2 | Bubble suspension concentrations in the contact zone. Conditions: saturator pressure 500 kPa, nitrogen enriched air in saturator, saturator efficiency 90%, 20°C, $k = 0$, d_b at 60 μm

R (%)	C_b (mg L^{-1})	Φ_b (ppm)	n_b (# L^{-1})
8	7.1	5,900	5.2×10^7
10	8.7	7,300	6.4×10^7
12	10.2	8,600	7.6×10^7

Table 3 | Ratios of bubble to floc volume and number concentrations for recycle ratio of 10% and floc volume of 21 ppm

Floc diameter (μm)	Φ_b/Φ_{floc}	n_b/n_{floc}
5	350	0.2
10	350	1.6
50	350	200

Downloaded from https://iwaponline.com/aqua/article-pdf/56/6-7/399/401152/399.pdf
by guest

BUBBLE AND FLOC-BUBBLE AGGREGATE RISE VELOCITIES

Bubbles

The classical Stokes equation (Equation (8)) is used to calculate rise velocities (v_b) of free bubbles – i.e., not attached to flocs. Bubble rise velocity depends greatly on bubble diameter (d_b), the density difference or driving force between water and air ($\rho_w - \rho_b$), and the water viscosity (μ_w). Figure 2 shows bubble rise velocities as a function of bubble diameter for cold (5°C) and warm water conditions (20°C). Obviously larger bubbles have greater rise rates than smaller ones, and bubbles rise faster in warmer water.

$$v_b = \frac{g(\rho_w - \rho_b)d_b^2}{18\mu_w} \tag{8}$$

For design of DAF tanks, water demands are greater in the summer or warm water conditions so rise velocities at 20°C is of interest. While bubbles in the contact zone have sizes mostly between 40 and 80 μm, which have rise velocities between 3.1 and 12.5 m h^{-1} (Figure 2), our main interest is the separation zone. There is evidence that the bubbles in the separation zone are larger than in the contact zone (Haarhoff & Edzwald 2004; Leppinen & Dalziel 2004), and a bubble diameter of 100 μm is a good estimate for the separation zone. The rise velocity for 100 μm bubbles is about 20 m h^{-1} (Figure 2). This serves as a reference value for the rise velocity of free bubbles in the separation zone.

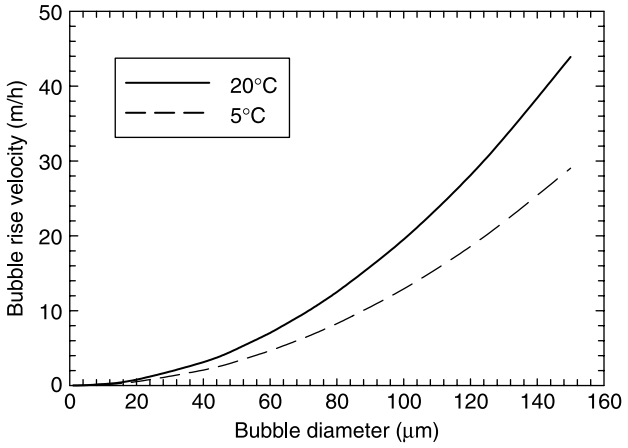

Figure 2 | Bubble rise velocities as a function of bubble size for 5 and 20°C.

Floc-bubble aggregates

The rise velocity of floc-bubble aggregates is calculated using the following equations, where d_{fb} is the aggregate equivalent diameter produced from N bubbles of size d_b attached to a floc particle of size d_p. ρ_{fb}, and v_{fb} are the floc-bubble aggregate density and aggregate rise velocity. K accounts for floc shape and drag force. For spheres, K is 24 (Haarhoff & Edzwald 2004). Here, it is assumed that K is 24 for flocs smaller than 40 μm, and increases gradually to 45 at a floc size at or above 170 μm.

$$d_{fb} = \left(d_f^3 + Nd_b^3\right)^{1/3} \tag{9}$$

$$\rho_{fb} = \frac{\rho_f d_f^3 + N\rho_b d_b^3}{d_f^3 + Nd_b^3} \tag{10}$$

$$v_{fb} = \frac{4g\left(\rho_w - \rho_{fb}\right)d_{fb}^2}{3K\mu_w} \tag{11}$$

The maximum number of bubbles that can possibly attach to a floc depends on the floc and bubble areas according to Tambo *et al.* (1986). For practical and conservative reasons, half the maximum number is allowed to attach in the following analysis. Thus, 1 bubble attachment occurs for flocs < 110 μm. The number of bubbles attached per floc increases gradually from 2 bubbles for flocs of 110 μm to 6 bubbles per floc for flocs of 200 μm. Figure 3 presents the results for the floc–bubble

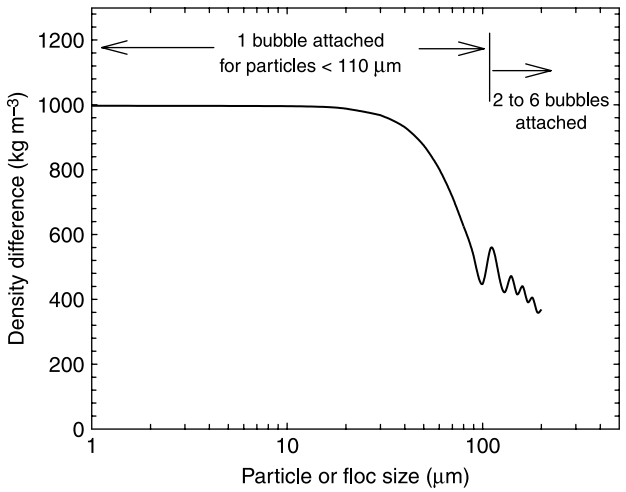

Figure 3 | Floc bubble aggregate density difference ($\rho_w - \rho_{fb}$) versus particle size with 1 bubble attachment for particles less than 110 μm and an increase in the number of bubbles attached for larger particles (Conditions: d_b of 100 μm; ρ_f of 1,100 kg m^{-3}, 20°C).

Downloaded from https://iwaponline.com/aqua/article-pdf/56/6-7/399/401152/399.pdf
by guest

aggregate density difference ($\rho_w - \rho_{fb}$) as a function of particle or floc size. The density difference represents conceptually the driving force for flotation. For floc-bubble aggregates to float, the density difference must exceed 0 and its maximum value (998.23 – 1.19) is approximately 1,000 kg m^{-3}. The maximum value occurs when the bubble size dominates compared to the floc or particle size so the ρ_{fb} is about equal to ρ_b, and so the driving force is approximately equal to that of free bubbles.

Whether a floc is small or large is relative to the bubble size of 100 μm. For a single 100 μm bubble attached to small size flocs of 50 μm or less, the aggregate density difference is close to the maximum value of 1,000 kg m^{-3} (value for free bubbles) because the bubble volume dominates, and the driving force for flotation is therefore large. The aggregate density difference decreases for single bubble attachment to flocs between 50 and about 100 μm (see Figure 3). Multiple bubble attachment can occur for larger flocs thereby maintaining a density difference of ~400 to 500 kg m^{-3} (Figure 3).

The floc-bubble aggregate rise velocity (v_{fb}) is now addressed, and the calculations displayed in Figure 4. Aggregate rise velocities are 20 m h^{-1} for flocs of 50 μm or less with just one bubble attached. Note that because the bubble volume (100 μm bubbles) dominates the particle volume (particles < 50 μm), the aggregates rise at about the same velocity of 20 m h^{-1} (reference value from above) as a 100 μm free bubble. As flocs increase in size from 50 to about 100 μm, the rise velocity decreases to about 10 m h^{-1} for 1 bubble attachment. Multiple bubble attachment can occur for flocs > 100 μm increasing the floc-bubble aggregate rise velocity. With 6 bubbles attached to a 200 μm floc, the aggregate rise velocity exceeds 20 m h^{-1} (Figure 4).

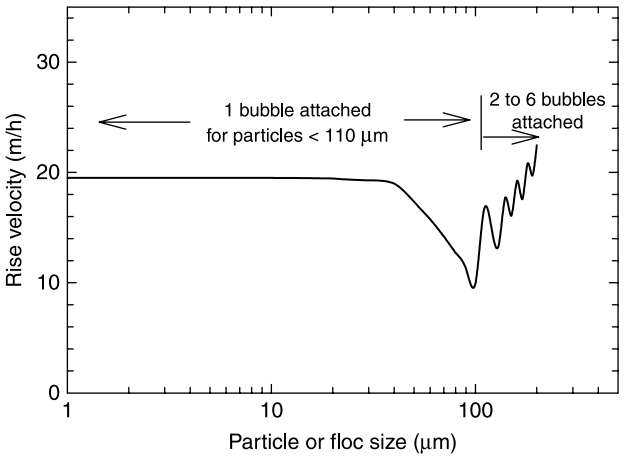

Figure 4 | Rise velocity of floc-bubble aggregates versus particle size with 1 bubble attachment for particles less than 110 μm and an increase in the number of bubbles attached for larger particles (Conditions: d_b of 100 μm; ρ_f of 110 kg m^{-3}, 20°C).

Since flocs of 200 μm and greater would most likely settle as they leave the flocculation tank, we assess flocs less than this size in evaluating the rise rates of aggregates. What we learn is that rise rates of free bubbles of 100 μm are about 20 m h^{-1}, and floc-bubble aggregates have about the same rise velocity for flocs < 50 μm with one bubble attached per floc. What is the optimum floc size for DAF? In the contact zone of the DAF tank, flocs of 10 s of microns are desired (see section, Description of Dissolved Air Flotation). For the separation zone, we found above that the maximum rise rate of 20 m h^{-1} is obtained with just 1 bubble attached per floc for flocs < 50 μm. Considering then the performance of both the contact and separation zones, it is concluded that the optimum floc sizes for DAF are about 20 to 50 μm.

DAF PERFORMANCE

Hazen theory for simple vertical flow through the separation zone

The separation zone of the DAF tank (see Figure 1) allows for gravity removal of free bubbles and floc-bubble aggregates. In practice, separation zone performance and design are based on Hazen theory. If we consider plug flow through the DAF tank separation zone in a vertical downward direction, then the rise velocities of the bubbles (v_b) and aggregates (v_{fb}) must exceed the separation zone hydraulic loading according to Equations (12) and (13) for removals of bubbles and aggregates.

$$v_b \geq v_{sz-hl} = \frac{Q + Q_r}{A_{sz}} \tag{12}$$

$$v_{fb} \geq v_{sz-hl} = \frac{Q + Q_r}{A_{sz}} \tag{13}$$

Prior to the 1990s, DAF tanks were designed at about 6 to 12 m h^{-1} based on separation zone hydraulic loadings (v_{sz-hl}). Even though these systems do not have vertical plug flow conditions, these designs were conservative and performed well because the loadings are much less than the bubble and aggregate rise velocities of say 20 m h^{-1}. Since the mid 1990s

Downloaded from https://iwaponline.com/aqua/article-pdf/56/6-7/399/401152/399.pdf
by guest

however, DAF tanks are being designed at high hydraulic loadings, even greater than 20 m h^{-1} and performing well. This means that the simple view depicted above is inadequate in predicting separation zone performance. I will revisit this matter below, but first some pilot data are presented illustrating DAF performance at high hydraulic loadings.

DAF pilot data at high hydraulic loadings

Edzwald *et al.* (1999) demonstrated through pilot studies that DAF can operate at high hydraulic loadings. One set of data from their studies is presented in Figure 5. These data show DAF effluent turbidities for hydraulic loadings of 21, 29, and 40 m h^{-1}. Two turbidity measurements were made to distinguish between particles and bubbles (bubble carryover) in the DAF effluent. The data show excellent DAF performance for particles with turbidities <0.4 NTU at all hydraulic loadings. At 21 m h^{-1} there is little bubble carryover, but the amount of bubbles in the effluent increased at higher hydraulic loadings, particularly at 41 m h^{-1}. The bubble carryover, however, did not affect granular media filtration performance following DAF. Filtered water turbidities were <0.1 NTU and head loss was not affected as unit filter run volumes were about 400 m^3/m^2, indicating good filter run times and production. Edzwald *et al.* (1999) also discussed methods to reduce bubble carryover. One method is to provide surfaces (tubes) in the tank to increase the separation zone area for removal of bubbles. Another way is to improve the hydraulic flow patterns through the tank. Examples are given in the next section.

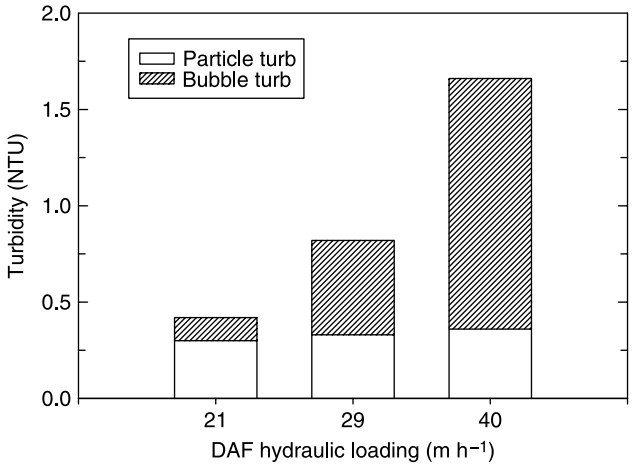

Figure 5 | DAF effluent turbidity due to particles and bubbles as a function of hydraulic loading (Pilot plant data for Hemlocks Reservoir, Fairfield, CT (USA), water temperature 12–17°C).

It is important to note that bubble carryover from DAF does not cause air binding in filters. Air binding in filters is caused by pressure reduction within the filter causing dissolved air to precipitate within the filter media. This results in large air bubbles that occupy the pore space between grains producing air binding. Most bubbles that may be in the DAF effluent from high rate processes never enter the filter box in full-scale plants. They are removed as water moves in channels and over weirs on the way to the filters. Within the filter box, most of those do not enter the filter media but will rise to the surface.

Developments in DAF equipment

In the last 5–10 years water treatment process companies have improved DAF equipment so DAF can be designed and operated at 20 to 40 m h^{-1} with excellent turbidity and particle removals and little or no bubble carryover. One system was developed by Rictor Oy (Finland), and it has been used by several drinking water plants. One plant of note is at Tampere (Finland), which was designed at about 40 m h^{-1}. In the USA there are plants in New York and California designed at least at 30 m h^{-1}. The Rictor technology is available for use around the world by license to Infilco Degrémont, and is known by the trade name of AquaDAF™. The AquaDAF™ system is depicted in the top part of Figure 6. The DAF tank operates at a high rate with improved hydraulic flow through the tank compared to many conventional tanks. A key development is the orifice plate floor at the bottom of the DAF tank that produces better flow distribution in the separation zone and at the outlet through the plate floor.

Amato *et al.* (2001) and Dahlquist & Göransson (2004) have reported on the development and application of a high rate DAF process, called DAFRapide®, which was developed by Purac Ltd. (UK) and Purac AB (Sweden). The DAFRapide®system is designed for high hydraulic loadings up to about 40 m h^{-1}, and it is depicted at the bottom of Figure 6. Internal tubes or plates may be placed in the DAF tank to improve the hydraulic flow distribution and to increase the separation zone area for improved removal of floc-bubble aggregates and free bubbles. Another feature of DAF Rapide® is that the DAF tank can perform well in drinking water applications utilizing short flocculation times of about 5 min. Finally, Leopold Company

Downloaded from https://iwaponline.com/aqua/article-pdf/56/6-7/399/401152/399.pdf
by guest

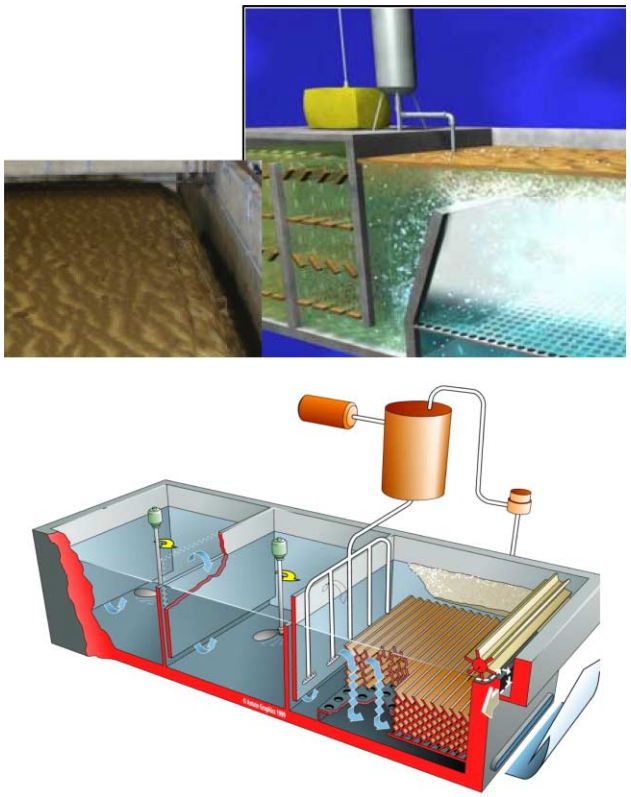

Figure 6 | High rate DAF systems. Top figure: AquaDAF℠ Infilco Degrémont (courtesy of Bob Raczko, United Water), note orifice plate floor; Bottom figure: DAFRapide® (courtesy of Enpure Ltd. (formerly, Purac) may contain tubes or plates).

has recently introduced a high rate DAF process known as Clari-DAF™.

Modification of the flow pattern through the separation zone for high rate DAF performance

High rate DAF systems are designed and operated at hydraulic loadings of 20 to 40 $m\,h^{-1}$. According to the Hazen theory described above in which the flow through the separation zone was considered plug flow in the vertical direction, these hydraulic loadings exceed bubble and aggregate rise velocities and these high rate DAF systems should not perform well, but they do.

One must consider the flow pattern through the separation zone. DAF tanks, especially those with higher hydraulic loadings exhibit stratified flow in which the flow moves horizontally along near the top of the separation zone to the end wall and then returns below this in a horizontal flow layer and may again reverse direction in a horizontal layer before proceeding to the exit at the tank bottom (Kiuru 2000; Lundh *et al.* 2000). A simple and conceptualized illustration of this stratified flow is shown in Figure 7. What is depicted shows two horizontal paths (could be more) followed by a vertical path. This depicted flow pattern effectively triples the clarification separation area, thereby reducing the equivalent clarification hydraulic loading ($v_{clar-hl}$) for separation of free bubbles and aggregates. Equations (12) and (13) are then modified to reflect the clarification area as expressed now by Equations (14) and (15).

$$v_b \geq v_{clar-hl} = \frac{Q + Q_r}{3(A_{sz})} \tag{14}$$

$$v_{fb} \geq v_{clar-hl} = \frac{Q + Q_r}{3(A_{sz})} \tag{15}$$

In this illustration of three flow paths, the equivalent clarification hydraulic loading ($v_{clar-hl}$) is 1/3 the separation zone hydraulic loading (v_{sz-hl}). Therefore, a DAF tank designed with a separation zone hydraulic loading of 40 $m\,h^{-1}$, will have a clarification hydraulic loading ($v_{clar-hl}$) of 40/3 or 13.3 $m\,h^{-1}$, which is less than expected rise velocities (v_b and v_{fb}) of 20 $m\,h^{-1}$.

Although the flow patterns through DAF tanks vary with hydraulic loading, recycle rate, and tank geometry, these considerations of stratified flow and the use of the clarification area hydraulic loading ($v_{clars-hl}$) explain why DAF tanks with hydraulic loadings >20 $m\,h^{-1}$ can perform well. Stratified flow effectively increases the area for

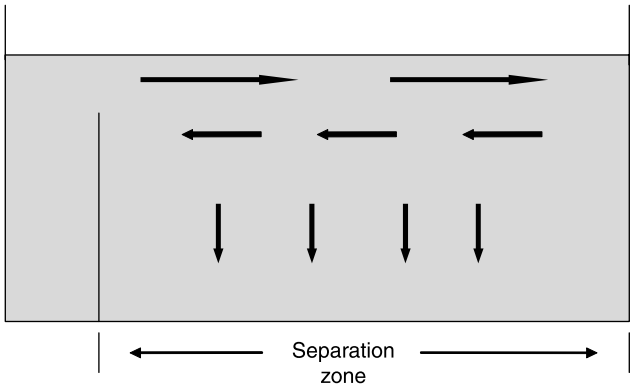

Figure 7 | Conceptualized stratified flow in high rate DAF processes.

Downloaded from https://iwaponline.com/aqua/article-pdf/56/6-7/399/401152/399.pdf
by guest

clarification, and is analogous to inserting trays (floors) in a sedimentation tank.

CONCLUSIONS

It is instructive to examine the bubble and floc particle concentrations in the contact zone of the DAF tank where bubbles and flocs undergo collisions and attachment to form floc-bubble aggregates. Bubble concentrations in terms of volume and number concentrations are about 6,000–9,000 ppm and $5–8 \times 10^7$ bubbles per L, respectively. Floc concentrations are highly dependent on the initial primary particle concentration and size, and on the extent of flocculation. For reservoir water applications, it is important to form flocs with sizes exceeding 10 s of microns so floc particle number concentrations are 10^6 flocs per L or less. As a result bubble volume and numbers exceed floc volumes and numbers, and thus insure adequate opportunities to form floc-bubble aggregates with density less than water.

The removals of bubbles and floc-bubble aggregates occur in the separation zone of the DAF tank. Bubble rise rates for 100 μm bubbles are $\sim 20\,m\,h^{-1}$. Floc-bubble aggregate rise velocities are at about their maximum value of $20\,m\,h^{-1}$ for flocs of 50 μm or less with just one bubble attached. As flocs increase in size the aggregate rise velocity decreases unless there is multiple bubble attachment. Multiple bubble attachment is required for flocs >100 μm to achieve rise velocities of 10 to $20\,m\,h^{-1}$.

Conventional DAF tanks were initially designed at hydraulic loadings of $5–10\,m\,h^{-1}$, and then increased in the 1990s to $10–15\,m\,h^{-1}$. These hydraulic loadings are less than the predicted rise velocities of bubbles and aggregates, thus linking rise velocities to hydraulic loadings through the Hazen theory for DAF tank separation zone performance. Since the 1990s, DAF processes have been designed at higher hydraulic loading rates. In the last several years, high rate DAF systems have been introduced with hydraulic loading rates of 20 to $40\,m\,h^{-1}$. The simple Hazen theory, which assumes plug flow in a vertical direction, is inadequate for predicting the removal of bubbles and aggregates for these high rate systems. It is shown that for high rate systems the flow through the separation zone is stratified, and this stratified flow pattern must be accounted for in relating separation zone efficiency to the hydraulic loading and bubble or floc-bubble aggregate rise rates. A conceptualized stratified flow model is used to explain why DAF tanks can be designed with hydraulic loadings $>20\,m\,h^{-1}$.

ACKNOWLEDGEMENTS

I am indebted to my former graduate students who have conducted research on dissolved air flotation over the past 20 years. I thank M. Kelley, J. Malley, A. Paralkar, D. Pernitsky, J. Plummer, K. Berger, K. Boudreau, S. Bullock, D. Bunker, M. Janay, S. Olson, L. Parento, W. Parmenter, C. Tamulonis, C. Udden, M. Valade, J. Walsh, B. Wingler, and C. Yu. The paper is based on a presentation made at the 7th International Symposium on Water Supply Technology held in Yokohoma, Japan, from 22 to 24 November 2007. The author made the presentation as Professor Emeritus, University of Massachusetts. He is now affiliated with Clarkson University as a Visiting Professor.

REFERENCES

Amato, T., Edzwald, J. K., Tobiason, J. E., Dahlquist, J. & Hedberg, T. 2001 An integrated approach to dissolved air flotation. *Water Sci. Technol.* **43**(8), 19–26.

Crossley, I. A. & Valade, M. T. 2006 A review of the technological developments of dissolved air flotation. *J. Water SRT – AQUA* **55**(7–8), 479–491.

Dahlquist, J. & Göransson, K. 2004 Evolution of a high rate dissolved air flotation process – from idea to full-scale application. In: Hahn, H., Hoffmann, E. & Ødegaard, H. (eds) *Chemical Water and Wastewater Treatment*. IWA Publishing, London, UK, pp. 297–308.

Edzwald, J. K., Malley, J. P. & Yu, C. 1990a A conceptual model for dissolved air flotation in water treatment. *Water Supply* **8**, 141–150.

Edzwald, J. K. & Wingler, B. J. 1990b Chemical and physical aspects of dissolved-air-flotation for the removal of algae. *J. Water SRT – AQUA* **39**(1), 24–35.

Edzwald, J. K., Walsh, J. P., Kaminsky, G. S. & Dunn, H. J. 1992 Flocculation and air requirements for dissolved air flotation. *J. AWWA* **84**(3), 92–100.

Edzwald, J. K. 1995 Principles and applications of dissolved air flotation. *Water Sci. Technol.* **31**(3–4), 1–23.

Edzwald, J. K., Tobiason, J. E., Amato, T. & Maggi, L. J. 1999 Integrating high rate dissolved air flotation technology into plant design. *J. AWWA* **91**(12), 41–53.

Downloaded from https://iwaponline.com/aqua/article-pdf/56/6-7/399/401152/399.pdf
by guest

Fukushi, K., Tambo, N. & Matsui, Y. 1995 A kinetic model for dissolved air flotation in water and wastewater treatment. *Water Sci. Technol.* **31**(3–4), 37–48.

Fukushi, K., Matsui, Y. & Tambo, N. 1998 Dissolved air flotation: experiments and kinetic analysis. *J. Water SRT – AQUA* **47**(2), 76–86.

Haarhoff, J. & Edzwald, J. K. 2001 Modelling of floc-bubble aggregate rise rates in dissolved air flotation. *Water Sci. Technol.* **43**(8), 175–184.

Haarhoff, J. & Edzwald, J. K. 2004 Dissolved air flotation modelling: insights and shortcomings. *J. Water SRT – AQUA* **53**(3), 127–150.

Han, M. 2002 Modeling of DAF: the effect of particle and bubble characteristics. *J. Water SRT – AQUA* **51**(1), 27–34.

Kiuru, H. J. 2000 *Proc. 4th Inter. Conf. on Dissolved Air Flotation in Water and Wastewater Treatment*, Helsinki.

Leppinen, D. M. & Dalziel, S. B. 2004 Bubble size distribution in dissolved air flotation tanks. *J. Water SRT – Aqua* **53**(8), 531–543.

Lundh, M., Jönsson, L. & Dahlquist, J. 2000 Experimental studies of the fluid dynamics in the separation zone in dissolved air flotation. *Water Res.* **34**(1), 21–30.

Matsui, Y., Fukushi, K. & Tambo, N. 1998 Modeling, simulation, and operational parameters of dissolved air flotation. *J. Water SRT – AQUA* **47**(1), 9–20.

Tambo, N., Matsui, Y. & Fukushi, K. 1986 A Kinetic Study of Dissolved Air Flotation. *World Congress of Chemical Engineering*, Tokyo, pp. 200–203.

Valade, M. T., Edzwald, J. K., Tobiason, J. E., Dahlquist, J., Hedberg, T. & Amato, T. 1996 Particle removal by flotation and filtration: pretreatment effects. *J. AWWA* **88**(12), 35–47.

First received 5 April 2007; accepted in revised form 19 June 2007

Downloaded from https://iwaponline.com/aqua/article-pdf/56/6-7/399/401152/399.pdf
by guest